Atmos. Chem. Phys. Discuss., 14, 15523–15543, 2014
www.atmos-chem-phys-discuss.net/14/15523/2014/
doi:10.5194/acpd-14-15523-2014

Atmospheric Chemistry and Physics Discussions
Open Access

Explicit representation of subgrid variability in cloud microphysics yields weaker aerosol indirect effect in the ECHAM5-HAM2 climate model

J. Tonttila[1,3], H. Järvinen[3], and P. Räisänen[2]

[1]Finnish Meteorological Institute, Atmospheric Research Centre of Eastern Finland, P.O. Box 1627, 70211 Kuopio, Finland
[2]Finnish Meteorological Institute, P.O. Box 503, 00101 Helsinki, Finland
[3]University of Helsinki, Department of Physics, P.O. Box 48, 00014 Helsinki, Finland

Received: 13 May 2014 – Accepted: 30 May 2014 – Published: 12 June 2014

Correspondence to: J. Tonttila (juha.tonttila@fmi.fi)

Published by Copernicus Publications on behalf of the European Geosciences Union.

Abstract

Impacts of representing cloud microphysical processes in a stochastic subcolumn framework are investigated, with emphasis on estimating the aerosol indirect effect. It is shown that subgrid treatment of cloud activation and autoconversion of cloud water to rain reduce the impact of anthropogenic aerosols on cloud properties and thus reduce the global mean aerosol indirect effect by 18 %, from 1.59 to 1.30 $\mathrm{W\,m^{-2}}$. Although the results show the importance of considering subgrid variability in the treatment of autoconversion, representing several processes in a self-consistent subgrid framework is emphasized. This paper provides direct evidence that omitting subgrid variability in cloud microphysics significantly contributes to the apparently chronic overestimation of the aerosol indirect effect by climate models, as compared to satellite-based estimates.

1 Introduction

Aerosol–cloud interactions and their changes due to anthropogenic aerosol emissions represent a major uncertainty in climate projections. In the Fifth Assessment Report (AR5) of the Intergovernmental Panel on Climate Change (IPCC), the uncertainty range for the effective radiative forcing due to aerosol-cloud interactions is given as −1.2 to 0.0 $\mathrm{W\,m^{-2}}$, with the best estimate at −0.45 $\mathrm{W\,m^{-2}}$, based on expert judgement supported by satellite studies (Boucher et al., 2013). The high uncertainty in this estimate stems to a large extent from the difficulty in separating the effects of aerosol-cloud interactions from other contributing feedbacks and processes. In addition, comparisons between general circulation models (GCM) and satellite studies have indicated that models typically overestimate the sensitivity of clouds to aerosol perturbations (Quaas et al., 2009). The median forcing value for estimates based on GCMs in AR5 (−1.4 $\mathrm{W\,m^{-2}}$) is indeed much larger in magnitude than the best estimate. The reasons for this overestimation are not fully understood.

ACPD
14, 15523–15543, 2014

The key topics in the model-based estimates of the aerosol indirect effects are those related to the parameterization of cloud microphysical processes, such as cloud activation of aerosols and the formation of drizzle and rain. Model representation of aerosol-cloud interactions and cloud droplet activation in particular has relied heavily on the use of parameterized effective vertical velocity in order to estimate the maximum supersaturation in a cloud layer for cloud droplet activation (Lohmann et al., 1999). This approach aims to provide a single, suitable vertical velocity value for the climate model grid cell, which is reminiscent of the typical small scale variability of the turbulent vertical motions. Tonttila et al. (2013) developed a more elaborate approach, where a stochastic subcolumn framework (Räisänen et al., 2004) was extended with subgrid vertical velocity samples drawn from a probability distribution. This enabled the calculation of the cloud droplet number concentration (CDNC) individually in each cloudy subcolumn, yielding an explicit representation of the variability of cloud structure and the distribution of the microphysical properties inside the climate model grid cells. The cloudy subcolumns can be directly used in the radiation calculations by the use of the Monte Carlo Independent Column Approximation method (MCICA; Pincus et al., 2003). This is a significant advantage, as now the entire chain of processes from formation of cloud droplets to radiative transfer can be considered consistently using the same subgrid framework. In addition, it provides an innovative approach for estimating the aerosol indirect effects, which is the main topic of this paper.

A series of climate model simulations using the modified model version from Tonttila et al. (2013) is presented in this study. These simulations are used to directly demonstrate that a significant part of the model-based overestimation of the aerosol indirect effect can be explained by omitting subgrid variability in cloud microphysical processes. A description of the model used in this study and the experimental setup is outlined in Sect. 2. Impacts of the subcolumn-based cloud microphysics on the present-day cloud properties are reported in Sect. 3. In Sect. 4, the impact of the subcolumn microphysics on the perturbation in cloud properties and radiation due to anthropogenic aerosol emissions is estimated, before drawing conclusions in Sect. 5.

ACPD
14, 15523–15543, 2014

2 Model description and experimental setup

The experiments in this study are performed using the ECHAM5-HAM2 aerosol-climate model (the model is thoroughly described in Roeckner et al., 2003, 2006; Zhang et al., 2012). The model version considered here has been modified to include the Monte Carlo Independent Column Approximation radiation scheme (Pincus et al., 2003) and a stochastic cloud generator (Räisänen et al., 2004, 2007) with the subgrid treatment of cloud microphysical processes (Tonttila et al., 2013). The model uses the large-scale condensation scheme by Tompkins (2002) to calculate the cloud fraction inside the GCM grid-box, and it also provides the statistical information about the subgrid variability of the total water amount needed by the stochastic cloud generator. To summarize the operation of the stochastic subgrid framework, subgrid columns created inside the GCM grid-columns by the stochastic cloud generator are used to describe the subgrid cloud structure and varying cloud condensate amount. Vertical velocity is assigned to each cloudy subcolumn based on samples drawn from a Gaussian probability density function (PDF) $P(\mu,\sigma)$, with the mean μ taken as the GCM grid-scale vertical velocity and the standard deviation given as $\sigma = 1.68\sqrt{\text{TKE}}$, where TKE is the turbulent kinetic energy provided by the GCM. The coefficient 1.68 is chosen in order to match the average magnitude of the vertical velocity from the subcolumn parameterization with the effective vertical velocity according to Lohmann et al. (2007), thus isolating the effect of explicit subgrid variability alone when comparing the results obtained using the two approaches (Tonttila et al., 2013). The subgrid vertical velocity samples from the PDF are used to calculate cloud droplet activation, which yields the distribution of CDNC in the subcolumn space. The parameterization used for cloud activation is that presented in Abdul-Razzak and Ghan (2000). Moreover, the autoconversion of cloud water into rain (Khairoutdinov and Kogan, 2000) can be treated separately for each subcolumn as well, since both liquid water content (LWC) and CDNC are known in the subcolumn space.

ACPD
14, 15523–15543, 2014

Three model configurations are used in this study, as summarized in Table 1. All of them use subgrid columns for radiation calculations, such that each layer of the subcolumns has a cloud fraction of 0 or 1, and cloud water content varies from one subcolumn to another (Räisänen et al., 2007). Furthermore, model closure parameters were not changed so that the only difference between the configurations is the treatment of cloud microphysics.

1. In REF, cloud droplet activation is computed using an effective vertical velocity (Lohmann et al., 2007). Consequently, subgrid-scale variations in CDNC are not considered. Furthermore, subgrid-scale cloud variability in LWC is considered in radiation calculations, but not in cloud microphysics.

2. In ACT, subgrid-scale variability of vertical velocity is considered in computing cloud activation, such that CDNC varies from one subcolumn to another. The width of the PDF for vertical velocity (σ) was fixed such that the sample mean value corresponds to the effective vertical velocity in REF (Tonttila et al., 2013). In contrast, autoconversion is evaluated based on the grid-mean values of LWC and CDNC, similarly to REF.

3. In ACACT, vertical velocity and cloud activation are calculated in the subcolumn space, similar to ACT. Furthermore, autoconversion is now also computed in the subcolumns, considering the subgrid-scale variations in LWC and CDNC.

A 5 year simulation for the years 2001–2005 was performed with configurations 1–3, each preceded by a 3 month spin-up. The simulations were nudged towards ERA-Interim reanalysis data (Dee et al., 2011) to suppress the impact of model internal variability, involving four model fields: vorticity (relaxation time scale 6 h), divergence (48 h), atmospheric temperature (24 h) and logarithm of surface pressure (24 h). The model horizontal resolution was T42 (corresponding to a grid-spacing of $\approx 2.8^{\circ}$) with 19 layers in the vertical. All simulations were run twice, separately with pre-industrial (PI) and present-day (PD) conditions in terms of aerosol emissions. These were obtained

ACPD
14, 15523–15543, 2014

J. Tonttila et al.

using the AEROCOM emission inventories (Dentener et al., 2006) for the years 1750 and 2000, respectively.

3 Impact of subgrid-scale parameterizations on cloud properties

In general, the differences between REF and ACACT for present-day conditions are similar to the results presented in Tonttila et al. (2013): adding subgrid treatment of cloud activation and autoconversion typically decreases CDNC and LWC, especially over industrialized areas. Nevertheless, a brief recap of these effects is presented since the model experiments in the current paper are run in the nudged configuration and the sensitivity of cloud properties to different parameterized components is analysed.

Figure 1 shows the zonal mean present-day cloud properties for the model experiments and observations, where available. Further, global mean values for related cloud parameters and the longwave and the sortwave cloud radiative effects for each model configuration are given in Table 2. The simulated vertically integrated cloud fraction (Fig. 1a) is higher than the observed (global mean at approximately 0.73 vs. 0.63 in the observations) especially at high latitudes and over the tropics, and similar between the different model configurations. The observations are from the International Satellite Cloud Climatology Project (ISCCP) D1 dataset (Rossow and Dueñas, 2004) averaged over the years 2001–2005. Note that the simulated cloud fraction is obtained using the ISCCP simulator (Klein and Jakob , 1999; Webb et al., 2001), which has been slightly modified in order to operate consistently with the subcolumns created by the stochastic cloud generator. Other modelling studies using ECHAM5 (without HAM2) with the Tompkins (2002) cloud cover scheme (e.g. Räisänen and Järvinen, 2010) show lower global cloud fraction than our experiments. Therefore the high total cloud cover appears to be an issue associated with the use of the HAM2 aerosol module together with the Tompkins (2002) cloud scheme. This issue is not influenced significantly by the inclusion of subgrid microphysics.

ACPD
14, 15523–15543, 2014

The liquid water path (LWP; Fig. 1b) is clearly decreased in ACACT as compared to both REF and ACT, which shows that the LWP is mostly controlled by the stronger autoconversion of cloud water to rain due to the subgrid treatment (Larson et al., 2001; Morales and Nenes, 2010; Tonttila et al., 2013). Instead, in the experiment ACT, LWP remains similar to REF in the Northern Hemisphere and is even slightly increased over southern mid-latitudes.

The zonal mean lower tropospheric CDNC sampled over land and oceans is shown in Fig. 1c and d, respectively. It is evident that subgrid treatment of cloud activation decreases the mean CDNC substantially, as indicated by the difference between ACT and REF. The largest difference occurs over land in the northern mid-latitudes, near the primary anthropogenic emission sources, while in more pristine regions, especially over the southern oceans, the differences are more modest. Tonttila et al. (2013) explained this behaviour by the modulated weighting caused by explicit subgrid variability in vertical velocity and its interaction with the aerosol size distribution, as the GCM grid-scale average magnitude of vertical velocity is kept similar regardless of the type of parameterization in our experiments. In the Southern Hemisphere and over the oceans, the low number of potential cloud condensation nuclei (CCN) is depleted at fairly low water vapour supersaturations, which reduces the sensitivity of cloud activation to vertical velocity variability. Therefore, explicitly accounting for the subgrid distribution of vertical velocity instead of using the effective value results in similar or even slightly increased CDNC. In comparison, in the northern mid-latitudes and especially over land, with higher CCN due to more numerous anthropogenic sources, the competition for water vapour between the potential CCN is stronger and the CDNC is more sensitive to the treatment of vertical velocity. Thus, the high frequency of occurrence of low vertical velocities in the subgrid distribution dominates in terms of CDNC, relative to the use of effective vertical velocity, which yields a decrease in the mean CNDC. Moreover, CDNC is even further reduced in ACACT as compared to ACT, owing to the enhancement of the autoconversion process due to subgrid treatment as mentioned above, which also influences the CDNC.

ACPD
14, 15523–15543, 2014

Contrasting the impacts seen on CDNC and LWP shows that the behaviour between the two is fairly consistent. In the Southern Hemisphere, the slightly increased CDNC shown by ACT over the oceans requires higher LWP for autoconversion to become effective, as compared to REF. In comparison, in the Northern Hemisphere subtropics and mid-latitudes, the CDNC is slightly lower for ACT especially over land, but LWP is similar to REF. This likely relates to the low sensitivity of autoconversion to small changes in CDNC in regions with high CCN concentration. Instead, for ACACT, the impact of subgrid treatment of autoconversion dominates the resulting LWP, for the most part masking out other effects.

The impact of the results above on the cloud optical properties are summarized by investigating the cloud optical depth. The zonal means of cloud optical depth (τ) calculated separately using data over land areas and over the oceans are shown in Fig. 1e and f, respectively (again using the ISCCP simulator). Observations in these figures are provided by the ISCCP dataset. Compared to REF, τ is clearly decreased in ACACT at all latitudes, with a larger difference over the oceans. The results from ACT are close to REF with a small increase in southern mid- and high latitudes over the oceans, and a slight decrease over Northern Hemisphere continents. The changes shown by both ACT and ACACT correspond well with the changes in LWP and CDNC discussed above. The comparison of the model results with ISCCP data shows that REF and ACT overestimate τ over the oceans and underestimate it over the continents. In ACACT, τ is underestimated over the continents as well, similar to REF and ACT. However, over the oceans, τ in ACACT agrees better with ISCCP data than the other experiments. The most outstanding improvements also coincide with the smallest bias in total cloud fraction (i.e., in the lower midlatitudes of each hemisphere), which makes this an encouraging result.

ACPD
14, 15523–15543, 2014

4 Anthropogenic aerosol effects

The impact of anthropogenic aerosols on cloud properties is evaluated as the difference between the PD and PI runs separately for each model configuration. The impact on CNDC at 890 hPa is considered in Fig. 2 and the impact on LWP in Fig. 3. Consistent with the distribution of anthropogenic emissions, the anthropogenic impacts on both the CDNC and the LWP are larger over the Northern Hemisphere than the Southern Hemisphere, in the vicinity of the main anthropogenic emission sources. The results show that subgrid treatment of the cloud microphysical parameterizations generally decreases the sensitivity of cloud properties to the anthropogenic aerosol perturbation.

For CDNC (Fig. 2), the weaker sensitivity to increasing aerosol concentration is easily visible in both ACT and ACACT as compared to REF. The global mean increase in CDNC between the PD and PI conditions is 30.7 cm^{-3} in ACACT and 31.8 cm^{-3} in ACT, which are clearly lower than the corresponding change in REF (36.4 cm^{-3}). Thus, the CDNC pertubation in ACACT is smaller than that in REF by 5.7 cm^{-3}. Most of this difference (about 80 %) is explained by the subgrid cloud droplet activation alone, as shown by ACT, while the type of treatment of autoconversion has only a minor impact on the global-mean anthropogenic CDNC perturbation. According to a two-tailed Student's t test, the difference between ACACT and REF is significant at the 99.9 % confidence level and that between ACT and REF at the 99 % level, while the difference between ACACT and ACT is not statistically significant. Thus, the type of treatment for autoconversion is not important for the anthropogenic perturbation in CDNC in our model.

Understanding why the anthropogenic perturbations in CDNC are decreased by subgrid cloud activation can be derived from the results in Sect. 3 and the discussion in Tonttila et al. (2013). The sensitivity of CDNC to subgrid variability of vertical velocity is highest in areas with high CCN concentration, where subgrid treatment of cloud activation acts to decrease the average number of activated droplets. Therefore, it can be expected that the substantial anthropogenic increase in CCN yields less increase

ACPD
14, 15523–15543, 2014

in CDNC in the experiment ACT than in REF. In addition, ACACT shows a small reduction in the anthropogenic CDNC perturbation as compared to ACT. This represents a feedback from the subgrid autoconversion on the mean CDNC, yet, as stated above, the difference is not statistically significant.

Perhaps a more meaningful view of the significance of the subgrid treatment of autoconversion is obtained through an examination of the anthropogenic impact on LWP. Similar to CDNC, subgrid variability in cloud microphysical parameterizations yields weaker increase in LWP due to anthropogenic aerosols. However, unlike for CNDC, REF and ACT show similar change in the global-mean LWP between PI and PD runs (7.62 and 7.63 $\mathrm{g\,m^{-2}}$, respectively), while the change in ACACT is 35 % weaker (4.96 $\mathrm{g\,m^{-2}}$). The difference in LWP response between ACACT and the two other simulations is significant at the 99.9 % confidence level. Accounting for subgrid variability in cloud microphysics therefore yields weaker anthropogenic perturbation in LWP, which is primarily due to accounting for the subgrid variability in CDNC and LWC in autoconversion and drizzle formation.

The aerosol indirect radiative effect is primarily estimated as the perturbation in the net cloud radiative effect (CRE) between the PI and PD simulations. This includes the combined effects of changing cloud lifetime, cloud extent and cloud albedo, but disregards the direct radiative effect of aerosols. The global mean indirect effect for each model configuration is given in Table 3, also separately for longwave and shortwave radiation. The net CRE perturbation for each model configuration is shown in Fig. 4. As expected based on the results for CDNC and LWC, ACACT promotes weaker global mean aerosol indirect effect ($-1.30\,\mathrm{W\,m^{-2}}$) compared to REF ($-1.59\,\mathrm{W\,m^{-2}}$). Interestingly, only a small difference is seen between ACT ($-1.52\,\mathrm{W\,m^{-2}}$) and REF, even though the anthropogenic increase in CDNC is significantly weaker over the industrialized areas. The differences in the radiative perturbation between ACACT and REF, and ACACT and ACT are significant at the 99.9 % level, while the difference between ACT and REF is not significant even at the 95 % confidence level. This result highlights the non-linearity inherent in the processes controlling the aerosol-cloud-radiation

ACPD
14, 15523–15543, 2014

interactions, which is now more accurately sampled since the different parameterizations from clouds to radiation are considered using the common subgrid framework. Although subgrid cloud activation alone has a relatively small impact on the aerosol indirect effect, it does influence the indirect effect when autoconversion is computed in the subcolumn space.

5 Conclusions

In this paper, we used the ECHAM5-HAM2 climate-aerosol model augmented with a stochastic subcolumn framework for cloud microphysics and radiation to study the aerosol indirect effects. Compared to a reference model configuration with GCM grid-scale cloud microphysics and thus uniform CDNC inside the GCM grid-cells, calculating cloud activation and autoconversion explicitly in the subcolumn space generally decreased the difference in cloud properties between pre-industrial (PI) and present-day (PD) aerosol emission conditions. In more detail, it was determined that subgrid treatment for cloud activation alone explained most of the decrease in anthropogenic perturbation of cloud droplet number concentration (CDNC) compared to GCM-scale microphysics. Adding subgrid treatment also for autoconversion had only a small impact on the CDNC perturbation between the PI and PD conditions, although it did yield lower global mean CDNC for the lower troposphere when examined separately for PI and PD model runs. For cloud liquid water path (LWP), the anthropogenic perturbation was reduced by the subgrid microphysics as well; however, now autoconversion had the largest effect, while subgrid cloud activation alone had a statistically insignificant impact. However, it should be noted that the subgrid treatment for cloud activation is one of the key elements in order to consider subgrid variability in the autocoversion process.

The indirect radiative effect of anthropogenic aerosols was investigated by analysing the perturbation in net cloud radiative forcing between the PI and PD conditions. Interestingly, with subgrid treatment for cloud droplet activation alone, the difference in the aerosol indirect effect to the reference simulation was relatively small. When both cloud droplet activation and autoconversion were considered in the subcolumn space, the anthropogenic perturbation in cloud radiative forcing was reduced by approximately 18 %. It has been documented that climate models in general tend to overestimate the magnitude of the indirect radiative effects of anthropogenic aerosols (Quaas et al., 2009), especially the interaction between the amount of aerosols and the cloud liquid water path. The results of this paper provide tangible evidence that omitting subgrid variability in the model representation of cloud microphysical properties significantly contributes to this overestimation.

Acknowledgements. This work was supported by a Väisälä foundation grant from the Finnish Academy of Science and Letters and by the Academy of Finland (project number 127210).

References

Abdul-Razzak, H. and Ghan, S. J.: A parameterization of aerosol activation .2. Multiple aerosol types, J. Geophys. Res., 105, 6837–6844, 2000. 15526

Boucher, O., Randall, D., Artaxo, P., Bretherton, C., Feingold, G., Forster, P., Kerminen, V.-M., Kondo, Y., Liao, H., Lohmann, U., Rasch, P., Satheesh, S. K., Sherwood, S., Stevens, B., Zhang, X. Y.: Climate Change 2013: The Physical Science Basis. Contribution of Working Group I to the Fifth Assessment Report of the Intergovernmental Panel on Climate Change, edited by: Stocker, T. F., Qin, D., Plattner, G.-K., Tignor, M., Allen, S. K., Boschung, J., Nauels, A., Xia, Y., Bex, V., and Midgley, P. M., Cambridge University Press, Cambridge, UK and New York, NY, USA, 2013. 15524

Dee, D. P., Uppala, S. M., Simmons, A. J., Berrisford, P., Poli, P., Kobayashi, S., Andrae, U., Balmaseda, M. A., Balsamo, G., Bauer, P., Bechtold, P., Beljaars, A. C. M., van de Berg, L., Bidlot, J., Bormann, N., Delsol, C., Dragani, R., Fuentes, M., Geer, A. J., Haimberger, L., Healy, S. B., Hersbach, H., Hólm, E. V., Isaksen, L., Kållberg, P., Köhler, M., Matricardi, M., McNally, A. P., Monge-Sanz, B. M., Morcrette, J.-J., Park, B.-K., Peubey, C., de Rosnay, P., Tavolato, C., Thépaut, J.-N., and Vitart, F.: The ERA-Interim reanalysis: configuration and performance of the data assimilation system. Q. J. Roy. Meteor. Soc., 137, 553–597, doi:10.1002/qj.828, 2011. 15527

ACPD
14, 15523–15543, 2014

Dentener, F., Kinne, S., Bond, T., Boucher, O., Cofala, J., Generoso, S., Ginoux, P., Gong, S., Hoelzemann, J. J., Ito, A., Marelli, L., Penner, J. E., Putaud, J.-P., Textor, C., Schulz, M., van der Werf, G. R., and Wilson, J.: Emissions of primary aerosol and precursor gases in the years 2000 and 1750 prescribed data-sets for AeroCom, Atmos. Chem. Phys., 6, 4321–4344, doi:10.5194/acp-6-4321-2006, 2006. 15528

Khairoutdinov, M. and Kogan, Y.: A new cloud physics parameterization in a large-eddy simulation model of marine stratocumulus, Mon. Weather Rev., 128, 229–243, 2000. 15526

Klein, S. A. and Jakob, C.: Validation and sensitivities of frontal clouds simulated by the ECMWF model, Mon. Weather Rev., 127, 2514–2531, 1999. 15528

Larson, V. E., Wood, R., Field, P. R., Golaz, J.-C., Haar, T. H. V., Cotton, W. R.: Systematic biases in the microphysics and thermodynamics of numerical models that ignore subgrid-scale variability, J. Atmos. Sci., 58, 1117–1128, 2001. 15529

Lohmann, U., Feichter, J., Chuang, C. C., and Penner, J. E.: Prediction of the number of cloud droplet in the ECHAM GCM, J. Geophys. Res., 104, 9169–9198, 1999. 15525

Lohmann, U., Stier, P., Hoose, C., Ferrachat, S., Kloster, S., Roeckner, E., and Zhang, J.: Cloud microphysics and aerosol indirect effects in the global climate model ECHAM5-HAM, Atmos. Chem. Phys., 7, 3425–3446, doi:10.5194/acp-7-3425-2007, 2007. 15526, 15527

Morales, R. and Nenes, A.: Characteristic updrafts for computing distribution-averaged cloud droplet number and stratocumulus cloud properties, J. Geophys. Res., 115, D18220, doi:10.1029/2009JD013233, 2010. 15529

Pincus, R., Barker, H. W., and Morcrette, J.-J.: A fast, flexible, approximate technique for computing radiative transfer in inhomogeneous cloud fields, J. Geophys. Res., 108, 4376, doi:10.1029/2002JD003322, 2003. 15525, 15526

Quaas, J., Ming, Y., Menon, S., Takemura, T., Wang, M., Penner, J. E., Gettelman, A., Lohmann, U., Bellouin, N., Boucher, O., Sayer, A. M., Thomas, G. E., McComiskey, A., Feingold, G., Hoose, C., Kristjánsson, J. E., Liu, X., Balkanski, Y., Donner, L. J., Ginoux, P. A., Stier, P., Grandey, B., Feichter, J., Sednev, I., Bauer, S. E., Koch, D., Grainger, R. G., Kirkevåg, A., Iversen, T., Seland, Ø., Easter, R., Ghan, S. J., Rasch, P. J., Morrison, H., Lamarque, J.-F., Iacono, M. J., Kinne, S., and Schulz, M.: Aerosol indirect effects – general circulation model intercomparison and evaluation with satellite data, Atmos. Chem. Phys., 9, 8697–8717, doi:10.5194/acp-9-8697-2009, 2009. 15524, 15534

Roeckner, E., Bäuml, G., Bonaventura, L., Brokopf, R., Esch, M., Giorgetta, M., Hagemann, S., Kirchner, I., Koernblueh, L., Manzini, E., Rhodin, A., Schlese, U., Schulzweida, U., and Tomp-

ACPD
14, 15523–15543, 2014

Aerosol effects in a subgrid framework

J. Tonttila et al.

kins, A.: The atmospheric general circulation model ECHAM5, Part I: model description, Rep. 349, Max Planck Institute for Meteorology, Hamburg, Germany, 127 pp., 2003. 15526

Roeckner, E., Brokopf, R., Esch, M., Giorgetta, M., Hagemann, S., Koernblueh, L, Manzini, E., Schlese, U., and Schulzweida, U.: Sensitivity of simulated climate to horizontal and vertical resolution in the ECHAM5 atmosphere model, J. Climate, 19, 3771–3791, 2006. 15526

Rossow, W. B. and Dueñas, E. N.: The International Satellite Cloud Climatology Project (ISCCP) web site, an online resource for research, B. Am. Meteorol. Soc., 85, 167–172, 2004. 15528

Räisänen, P. and Järvinen, H.: Impact of cloud and radiation scheme modifications on climate simulated by the ECHAM5 atmospheric GCM, Q. J. Roy. Meteor. Soc., 136, 1733–1752, doi:10.1002/qj.674, 2010. 15528

Räisänen, P., Barker, H. W., Khairoutdinov, M. F., Li, J., and Randall, D. A.: Stochastic generation of subgrid-scale cloudy columns for large-scale models, Q. J. Roy. Meteor. Soc., 130, 2047–2067, 2004. 15525, 15526

Räisänen, P., Järvenoja, S., Järvinen, H., Giorgetta, M., Roeckner, E., Jylhä, K. and Ruosteenoja, K.: Tests of Monte Carlo independent column approximation in the ECHAM5 atmospheric GCM, J. Climate, 20, 4995–5011, doi:10.1175/JCLI4290.1, 2007. 15526, 15527

Tompkins, A. M.: A prognostic parameterization for the subgrid-scale variability of water vapor and clouds in large-scale models and its use to diagnose cloud cover, J. Atmos. Sci., 59, 1917–1942, 2002. 15526, 15528

Tonttila, J., Räisänen, P., and Järvinen, H.: Monte Carlo-based subgrid parameterization of vertical velocity and stratiform cloud microphysics in ECHAM5.5-HAM2, Atmos. Chem. Phys., 13, 7551–7565, doi:10.5194/acp-13-7551-2013, 2013. 15525, 15526, 15528, 15529, 15531

Webb, M., Senior, C., Bony, S. and Morcrette, J.-J.: Combining ERBE and ISCCP data to asses clouds in the Hadley Centre, ECMWF and LMD atmospheric climate models, Clim. Dynam., 17, 905–922, 2001. 15528

Zhang, K., O'Donnell, D., Kazil, J., Stier, P., Kinne, S., Lohmann, U., Ferrachat, S., Croft, B., Quaas, J., Wan, H., Rast, S., and Feichter, J.: The global aerosol-climate model ECHAM-HAM, version 2: sensitivity to improvements in process representations, Atmos. Chem. Phys., 12, 8911–8949, doi:10.5194/acp-12-8911-2012, 2012. 15526

Table 1. Experimental setup indicating whether the parameterized components marked on the top row are calculated in the GCM-scale (–) or in the subcolumn-space (+).

Experiment	Radiation	cloud activation	autoconversion
REF	+	–	–
ACT	+	+	–
ACACT	+	+	+

ACPD
14, 15523–15543, 2014

Table 2. Present-day global mean values in each model configuration for (from top to bottom) total cloud cover (C_{tot}), liquid water path (LWP), ice water path (IWP), CDNC burden, shortwave cloud radiative effect (SWCRE) and longwave cloud radiative effect (LWCRE).

	REF	ACT	ACACT
C_{tot}	73.5	73.8	72.8
LWP [$g\,m^{-2}$]	65.0	67.4	50.2
IWP [$g\,m^{-2}$]	7.1	7.0	7.0
CDNC burden [cm^{-2}]	3.96×10^6	3.77×10^6	2.86×10^6
SWCRE [$W\,m^{-2}$]	−55.92	−56.63	−52.75
LWCRE [$W\,m^{-2}$]	27.74	27.64	27.47

ACPD
14, 15523–15543, 2014

Table 3. Global mean aerosol indirect radiative effect in each model configuration given in terms of the shortwave (AIE_{SW}), longwave (AIE_{LW}) and net (AIE_{Net}) radiative forcing in $W\,m^{-2}$.

	REF	ACT	ACACT
AIE_{SW}	−1.82	−1.86	−1.56
AIE_{LW}	0.23	0.34	0.26
AIE_{Net}	−1.59	−1.52	−1.30

ACPD
14, 15523–15543, 2014

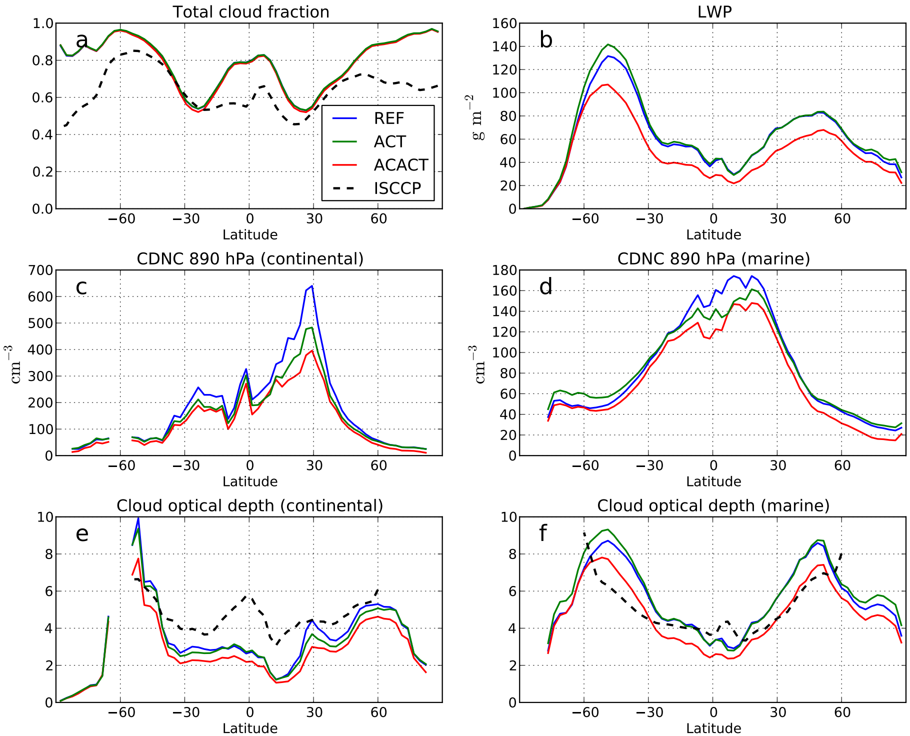

Figure 1. Zonal mean cloud properties for present-day conditions for different model configurations (summarized in Table 1) and observations from ISCCP. **(a)** Vertically integrated total cloud fraction, **(b)** liquid water path, **(c)** in-cloud CDNC at the 890 hPa level over land, **(d)** in-cloud CDNC at the 890 hPa level over the oceans, **(e)** cloud optical depth over land and **(f)** cloud optical depth over the oceans. Note that the ISCCP simulator was used to obtain the model estimates for **(a)**, **(e)** and **(f)**.

ACPD
14, 15523–15543, 2014

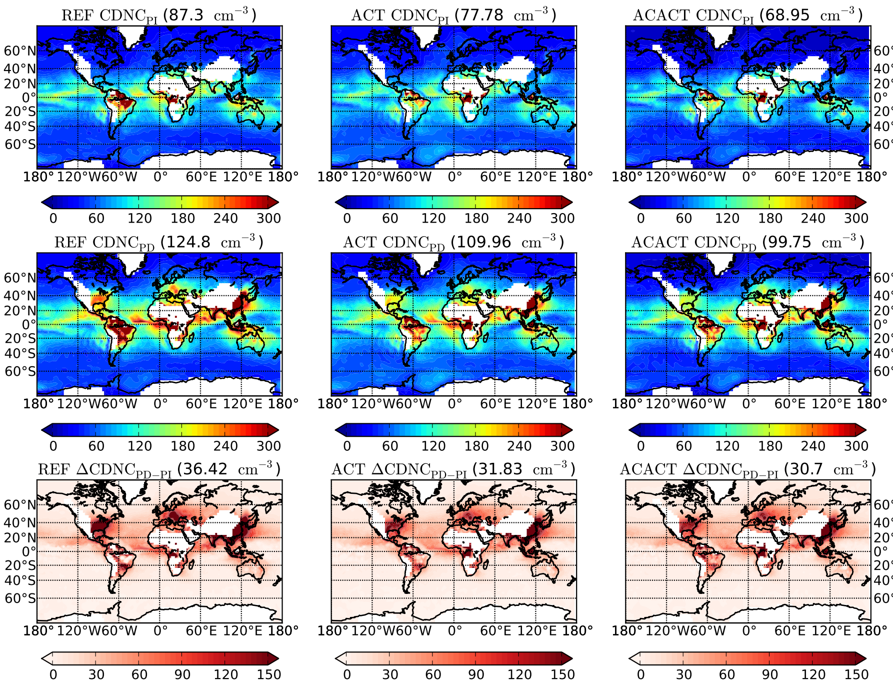

Figure 2. Comparison of in-cloud CDNC at the 890 hPa pressure level (cm^{-3}) between pre-industrial (PI) and present-day (PD) conditions for each model configuration as indicated in the panels. The global mean is given in the parentheses.

ACPD
14, 15523–15543, 2014

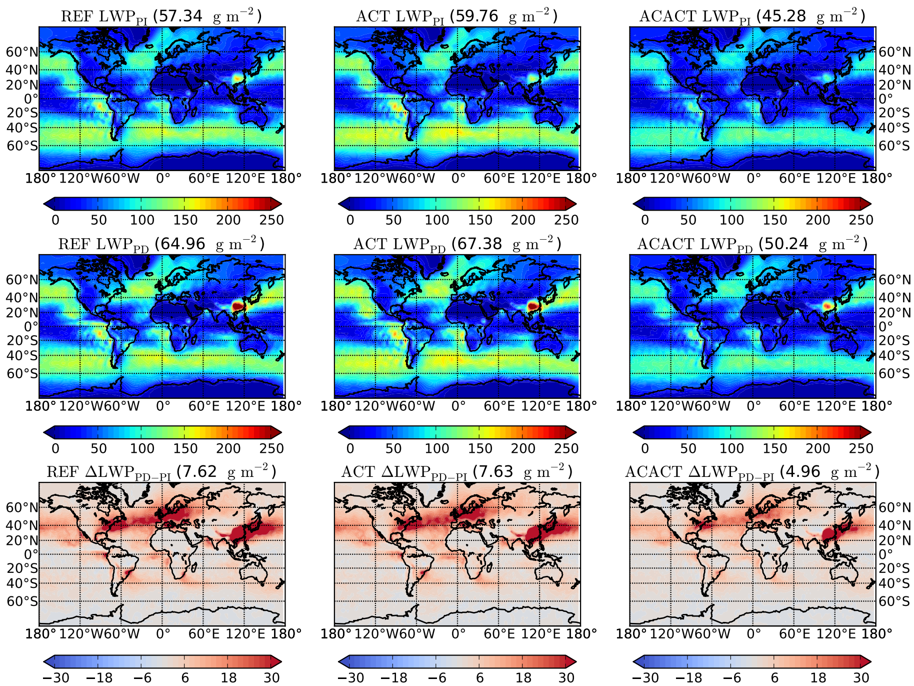

Figure 3. Comparison of the LWP (g m^{-2}) between pre-industrial (PI) and present-day (PD) conditions for each model configuration as indicated in the panels. The global mean is given in the parentheses.

ACPD
14, 15523–15543, 2014

Aerosol effects in a subgrid framework

J. Tonttila et al.

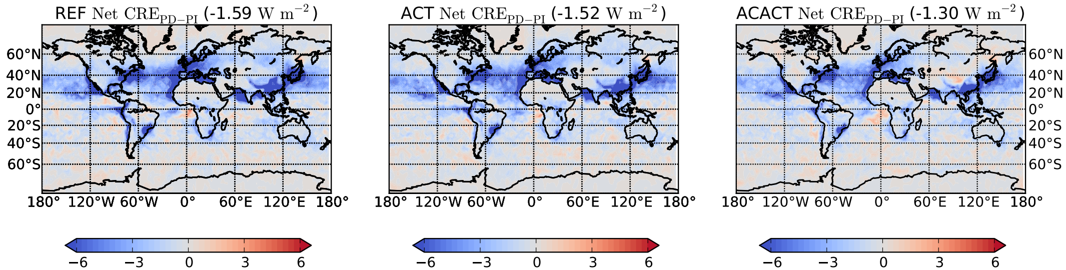

Figure 4. Aerosol indirect effects estimated as the perturbation in the net cloud radiative effect (Net CRE, W m^{-2}) between pre-industrial (PI) and present-day (PD) conditions for REF, ACT, and ACACT.

ACPD
14, 15523–15543, 2014

Aerosol effects in a subgrid framework

J. Tonttila et al.